JOURNAL OF MATERIALS SCIENCE 22 (1987) 4326–4330

Creep-sintering of zinc oxide

M. N. RAHAMAN*, L. C. DE JONGHE
Materials and Molecular Research Division, Lawrence Berkeley Laboratory, University of California, Berkeley, California 94720, USA

The simultaneous creep and densification of zinc oxide powder compacts was studied, using a loading dilatometer, at 725° C subjected to uniaxial stresses of up to 0.25 MPa. Between relative densities of 0.50 and 0.85, the dependence of the uniaxial creep rate on density can be described in terms of a stress intensification factor, ϕ, of the form $\phi \sim \exp(aP)$, where a is constant equal to 5.0 and P is the porosity. Comparison of the creep and densification rates showed that the ratio of the linear densification rate to the creep rate is nearly constant over a density range between 0.55 and 0.85, and permitted the evaluation of the sintering effective stress, which is found to decrease with increasing density. The results are compared with those obtained earlier for cadmium oxide and a soda-lime glass powder.

1. Introduction

It is now widely recognized that heterogeneities (e.g. hard agglomerates, particle or fibre inclusions) present in a powder compact lead to non-uniform local sintering rates which, in turn, produce transient stresses [1–4]. Unless these stresses are relieved by creep processes, they can lead to a reduction in densification rates, and may even cause microcracking in the sintering compact. Clearly, a fundamental parameter for a powder system is the relative magnitude of the densification rate to the creep rate.

The technique of loading dilatometry [5] was developed by the present authors to quantify the interaction between creep and densification during sintering. Basically, a controlled, measured uniaxial stress is applied to the sintering compact. For applied stresses much less than the sintering stress or for creep strains much smaller than the linear densification strain, creep and densification can be treated as independent processes, as found in earlier work on CdO [6, 7].

Earlier papers by the present authors using CdO [6, 7] explored the usefulness of the loading dilatometer technique and the analysis of the experimental data to evaluate the functional dependence of the stress intensification factor, ϕ, [9–12] and the sintering stress, Σ/ϕ, [14, 15], on density and grain size. Experiments have also been performed on magnesium oxide [16] and soda-lime glass powder [8]. The only other published work on the effect of uniaxial (or shear) stress on densification has been performed by Venkatachari and Raj [16] on alumina doped with about 0.25 wt % magnesium oxide. Venkatachari and Raj used stresses greater than the sintering stress. Although the creep strains ranged up to ~ 0.7 while the linear densification strain was less than ~ 0.15, their results indicated that creep and densification could still be treated as independent processes.

This paper reports on the simultaneous creep and densification behaviour of ZnO powder compacts. The results will be compared with those obtained earlier for CdO and a soda-lime glass powder. The results of these creep-sintering experiments are not only important for the understanding of fundamental issues in the sintering of single phase systems but are also of considerable value in accounting for the densification of heterogeneous powder compacts [15] and particulate composites [3, 17, 18].

2. Experimental procedure

Zinc oxide powder (Reagent grade, Mallinckrodt Inc., Paris, Kentucky) compacts (6 mm diameter × 6 mm), having a green relative density of 0.45 ± 0.01 were made by uniaxial compaction of the powder at ~ 20 MPa in a tungsten carbide die. The average grain size of the powder was $\sim 0.4\,\mu$m. The compacts were sintered in flowing, dry air (50 $cm^3\,min^{-1}$) for 2 h in a loading dilatometer. The instrument and its associated control and monitoring equipment have been described in detail elsewhere [5, 6]. Sintering was performed at 725° C and under low, uniaxial stresses between 0 and 0.25 MPa. The sintering procedure was similar to that described earlier for CdO [6]. The mass and dimensions of the samples were measured before and after sintering and the final density measured using Archimedes' principle. In a separate set of experiments, sintering was terminated after times between 0 and 2 h, and the dimensions of these compacts measured using a micrometer.

The average grain sizes of three separate specimens were measured after sintering for 20, 60 and 120 min. Measurements were taken from scanning electron micrographs of polished and thermally etched samples. Samples were vacuum impregnated with epoxy resin and then polished using diamond paste and non-aqueous lubricants. A "flash-etching" method was used in order to minimize grain growth during the etching stage. Samples were first thermally equilibrated at 500° C, then rapidly inserted into the hot

Present address: University of Missouri-Rolla, Ceramic Engineering Department, Rolla, Missouri 65401, USA.

0022–2461/87 $03.00 + .12

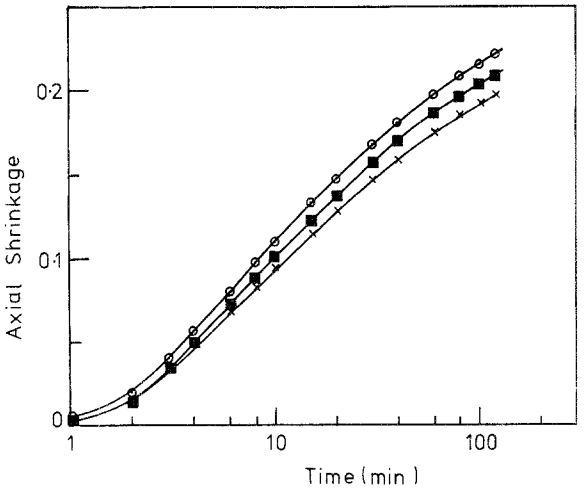

Figure 1 Axial shrinkage against time for ZnO compacts sintered under low applied loads at 725° C. Loads (×) 0 N, (■) 3.5 N, (○) 7 N.

zone of the furnace at 1000° C, and kept there for 30 sec, after which time they were rapidly removed. This technique produced a light etch that was adequate for delineating the grain boundaries. Grain sizes were measured by counting the number of grains traversed by straight lines of known length. The average grain size was taken as 1.5 times the average intercept length. Dihedral angles were obtained from micrographs of polished samples having a relative density of ~0.85.

3. Results

Fig. 1 shows the axial shrinkage, $\Delta L/L_0$, against time, t, for applied loads between 0 and 7 N (L_0 is the initial sample length and $\Delta L = L - L_0$, where L is the instantaneous sample length). A load of 1 N represents a stress of 35 kPa on the green, unsintered compact, and $t = 0$ represents the beginning of shrinkage. The sintering temperature (725° C) was reached after $t = 6$ min. Each curve is the average of two runs under the same conditions, and each is reproducible to within ±2%. Weight losses in the samples were less than 1% after 2 h at the sintering temperature, and the applied loads could be maintained to within ±5% for

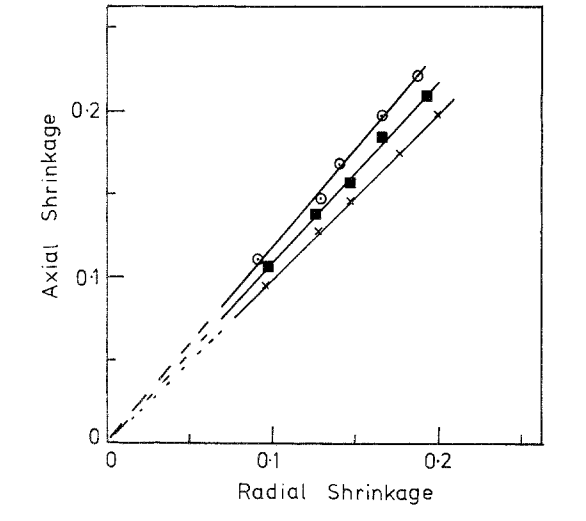

Figure 2 Axial shrinkage against radial shrinkage for compacts sintered under loads (×) 0 N, (■) 3.5 N, (○) 7 N.

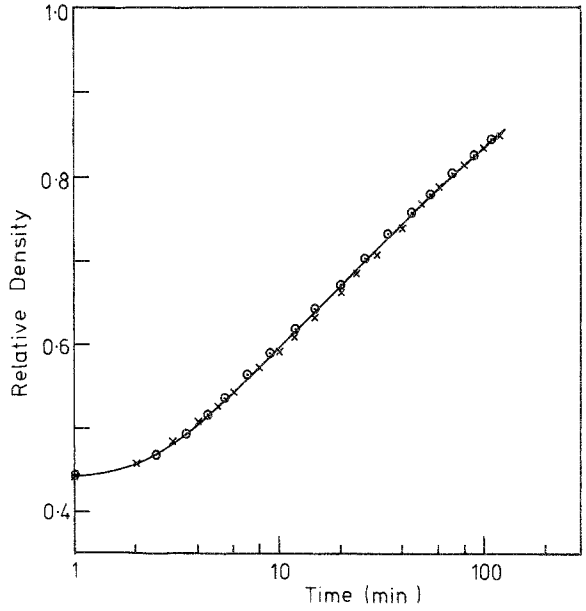

Figure 3 Relative density against time (×) 0 N, (○) 7 N.

the duration of the experiment. It is seen that at any time, t, the axial shrinkage increases with increasing load.

The application of a uniaxial load causes anisotropic shrinkage of the compact, as shown in Fig. 2, where $\Delta L/L_0$ is plotted against the radial shrinkage $\Delta d/d_0$ (d_0 is the initial sample diameter, and $\Delta d = d - d_0$, where d is the instantaneous sample diameter). The $\Delta L/L_0$ values are approximately proportional to $\Delta d/d_0$ and the slopes of the lines increase with increasing load.

The creep strain, ε, was separated from the volumetric densification strain using the results of Figs 1 and 2 and the methodology described by Raj [20]. Fig. 3 shows the relative density, ϱ, against log t for zero applied load and for the maximum applied load of 7 N. The curves for the other loads have been omitted for clarity. Similar to the results obtained for CdO [6, 7], the small loads cause almost no change in ϱ. The effect of applied load on the creep behaviour is shown in Fig. 4. It is seen that although ε increases with applied load, the creep strains are small (< 3%). Creep strains of this magnitude are expected to have no effect on the evolution of the pore morphology during creep-sintering.

The relative densification rate, $\dot{\varrho}$, and the creep rate,

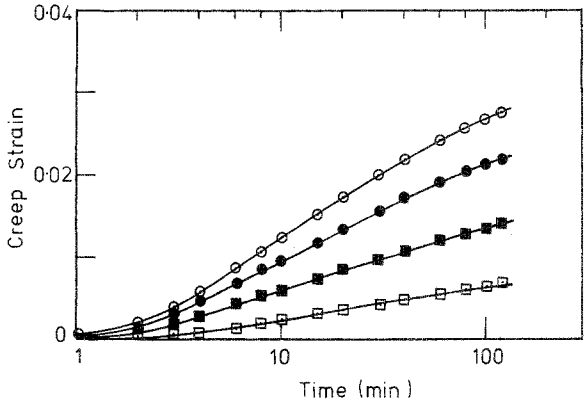

Figure 4 Creep strain against time for loads (□) 1.75 N, (■) 3.5 N, (●) 5 N, (○) 7 N.

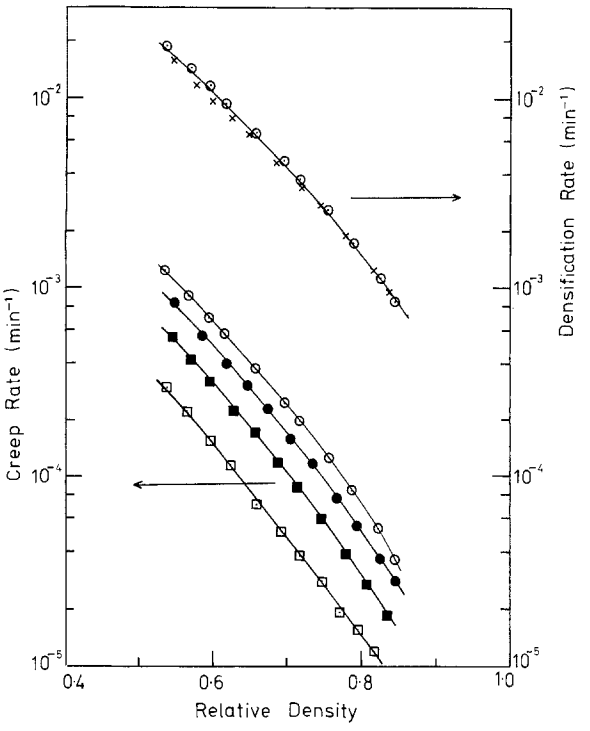

Figure 5 Densification rate, $\dot{\varrho}$, and creep rate, $\dot{\varepsilon}$, against relative density for applied stresses (×) 0 MPa, (□) 0.06, (■) 0.12, (●) 0.17, (○) 0.25.

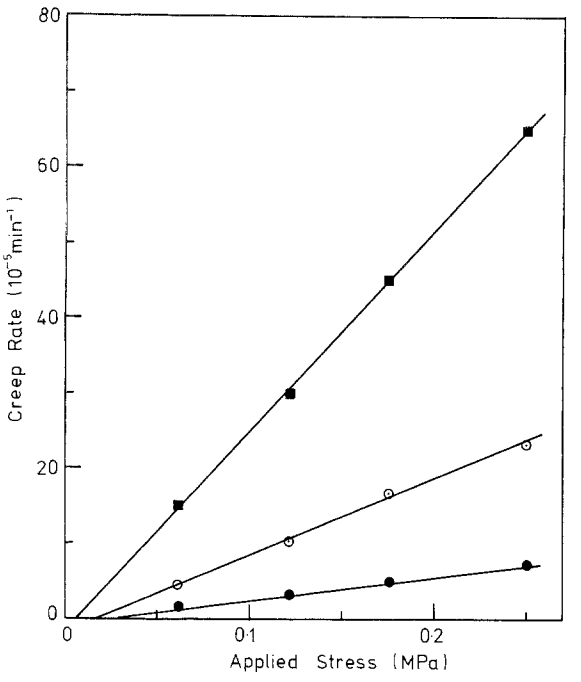

Figure 6 Creep rate against applied stress for relative densities (■) 0.6, (○) 0.7, (●) 0.8.

$\dot{\varepsilon}$, were obtained as a function of ϱ (or t) by fitting smooth curves to the results of Figs 3 and 4 and differentiating. However, to evaluate the results at constant applied stress, a small correction has to be made for the change in the cross-sectional area of the sample during the experiment, as outlined earlier [7].

Fig. 5 shows the results for $\dot{\varrho}$ and $\dot{\varepsilon}$ against ϱ at constant applied stresses. The curves for $\dot{\varrho}$ and $\dot{\varepsilon}$ have similar shapes and decrease approximately linearly with ϱ for values of ϱ between 0.5 and 0.8. Similar trends were obtained earlier for CdO [7]. The results for $\dot{\varepsilon}$ against the applied stress, σ_a, for relative densities between 0.6 and 0.8 are shown in Fig. 6. A linear dependence of $\dot{\varepsilon}$ on σ_a is found, and this indicates a diffusion mechanism for the creep process. The small negative intercept for $\dot{\varepsilon}$ for $\sigma_a = 0$ is due to a small amount of anisotropic densification in the die-pressed compact, i.e. for the sample sintered under no load, the radial shrinkage is slightly greater than the axial shrinkage.

Fig. 7 shows scanning electron micrographs of polished and etched samples sintered for 20 and 120 min. Grain growth is relatively small and the initial grain size of the compact increases by a factor of ~ 2 after sintering for 2 h. The increase in the grain size can be best fitted to a cubic growth law, Fig. 8, of the form $(G/G_0)^3 = 1 + kt$, where k is a constant equal to 0.05 and G_0 is the initial grain size. The mean value of the dihedral angle was $118 \pm 10°$.

4. Discussion

4.1. The stress intensification factor ϕ

As outlined earlier [7], the creep data may be treated in terms of a general equation of the form

$$\dot{\varepsilon} = \frac{CD\Omega\sigma_e^n}{GX_0^{m-1}k_BT} \quad (1)$$

where X_0 is the radius of a load-bearing grain bound-

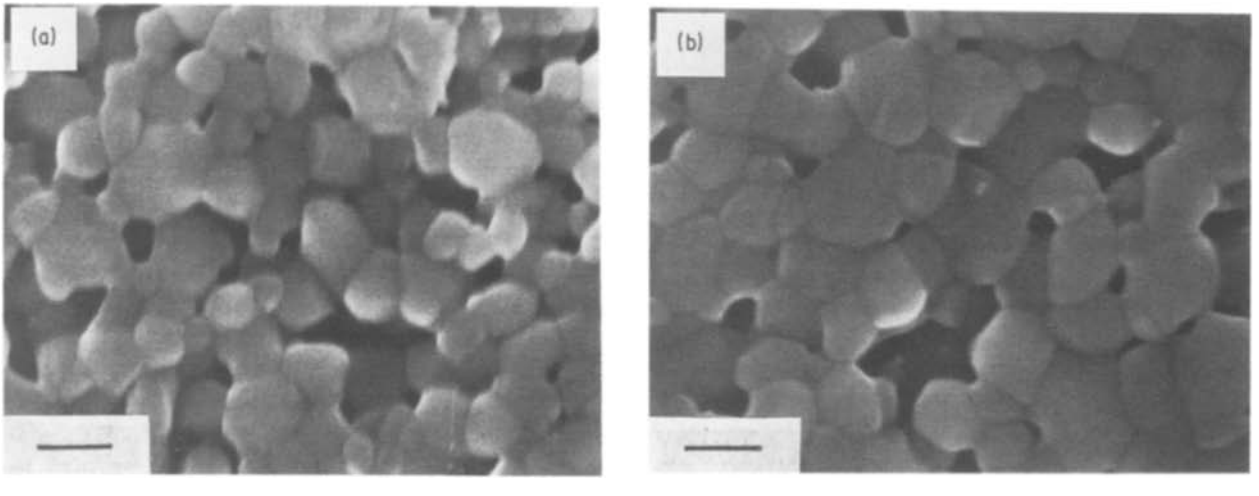

Figure 7 Scanning electron micrographs of polished and etched samples sintered for (a) 20 min and (b) 120 min. (Bar = 0.5 μm).

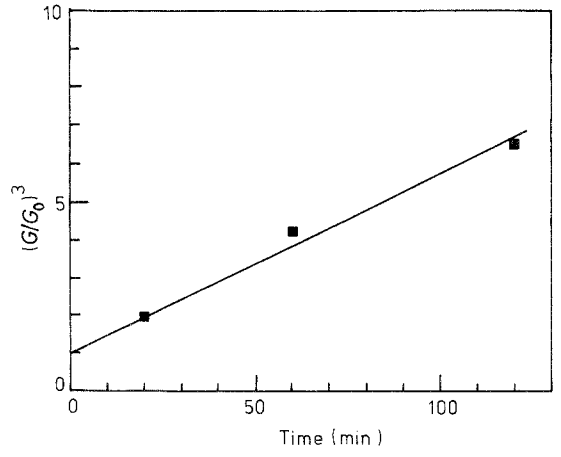

Figure 8 The cube of the grain size normalized to the initial grain size, $(G/G_0)^3$ against time.

ary area between two grains, or the pore spacing, C is a constant defined by the geometry, D is the diffusivity, Ω is the molecular volume, k_B is the Boltzmann constant, T is the absolute temperature, σ_e is the effective mean stress on the load-bearing parts of grain boundaries, and m and n are exponents characteristic of the creep mechanism. For diffusion-controlled creep $n = 1$, as observed here for ZnO. For lattice diffusion (Nabarro–Herring creep [20, 21], $m = 2$, while for grain boundary diffusion (Coble creep [22]), $m = 3$. According to Gupta and Coble [23], mass transport during sintering of ZnO occurs by lattice diffusion. For the low stresses used in these experiments the creep mechanism is expected to be similar to that for densification, so that $m = 2$. The stress intensification factor, ϕ, is defined as

$$\phi = (A/A_e) = (G/X_0)^2 \quad (2)$$

where A_e and A are the effective, load-bearing area and the total cross-sectional area respectively. For ZnO, Equation 1 may then be simplified to give

$$G^2\dot{\varepsilon} = K_1\sigma_a\phi^{3/2} \quad (3)$$

where K_1 is a constant at a fixed temperature. A plot of $G^2\dot{\varepsilon}$ against ϱ, as shown in Fig. 9, would then give the functional dependence of ϕ on ϱ. It is seen that ϕ is an exponential function of ϱ for values of ϱ between 0.55 and 0.85, i.e. $\phi = \exp(aP)$, where $a = 5.0$ and P the porosity ($P = 1 - \varrho$). The observed value of a is somewhat lower than the value $a = 6$ predicted by the Beere model [10–12] for the observed dihedral angle of $\sim 120°$. For CdO [7], with almost the same dihedral angle (125°), it was observed that $a = 2.0$.

Thus for both CdO and ZnO, the observed dependence of ϕ on porosity is stronger than that of the Coble expression [3] of $\phi \sim 1/\varrho$, but significantly weaker than that predicted by the Beere model [10, 11]. As pointed out by Vieira and Brook [12], the Coble expression may be more valid for $\varrho < 0.9$, i.e. for the final stage of densification when the pores are isolated, and nearly spherical. The observed deviation from the Beere model may originate from at least two main assumptions of the theory; first, that rapid surface relaxation occurs to produce equilibrium pore shapes, and second, that the number of pores per grain remains constant. The first assumption cannot, at present, be tested due to the lack of surface diffusion coefficients for CdO and ZnO, but the second is not completely valid since grain growth and pore size distributions can lead to a reduction in the average number of pores per grain.

4.2. The ratio of densification rate to creep rate

As outlined earlier, the ratio of the densification rate to the creep rate is of fundamental importance in the understanding of the sintering behaviour of composites and other heterogeneous systems. Fig. 10 shows the ratio of the linear densification rate to the creep rate, $\dot{\varrho}/3\varrho\dot{\varepsilon}$, against ϱ. This ratio was evaluated at a constant applied stress of 0.25 MPa.

It is seen that $\dot{\varrho}/3\varrho\dot{\varepsilon}$ is approximately constant over density range between 0.55 and 0.85. This ratio has also been found to be nearly constant with density for CdO and a soda-lime glass powder [8, 24].

4.3. The sintering effective stress, Σ

Following Equation 3, the expression for the densifi-

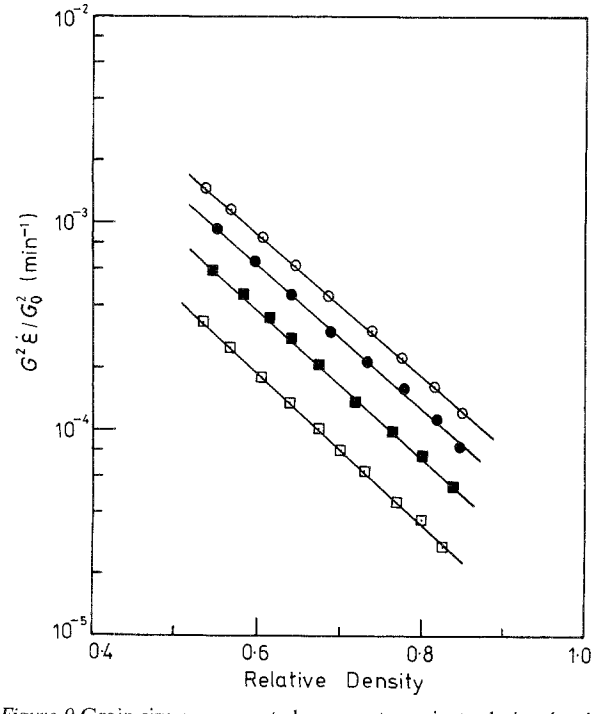

Figure 9 Grain size compensated creep rate against relative density for applied stresses (□) 0.06, (■) 0.12, (●) 0.17, (○) 0.25.

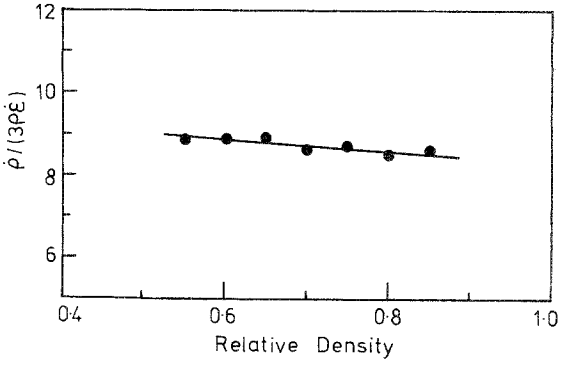

Figure 10 Ratio of linear densification rate to creep rate against relative density.

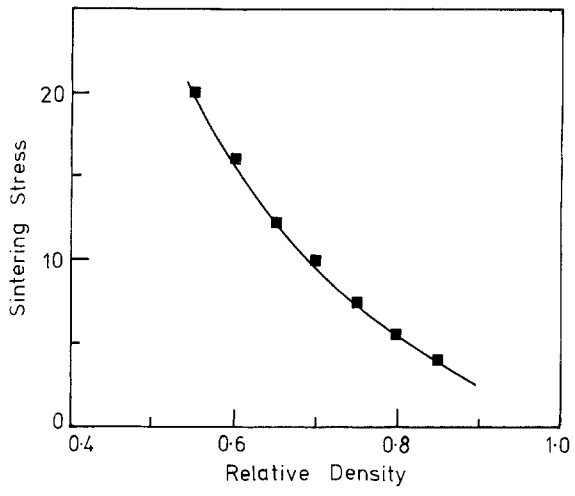

Figure 11 Sintering effective stress against relative density.

cation rate may be written as

$$G^2\dot{\varrho} = K_2\Sigma\phi^{1/2} \quad (4)$$

where K_2 is a constant, Σ is the effective sintering stress, and the densification mechanism is lattice diffusion. Then from Equations 3 and 4

$$(\dot{\varrho}/3\varrho\dot{\varepsilon}) = (K_1/K_2)\Sigma/(\sigma_a\phi) = K_3\Sigma/(\sigma_a\phi) \quad (5)$$

where K_3 is a constant. Since $(\dot{\varrho}\beta\varrho\dot{\varepsilon})$ has been observed to be relatively constant, then the most significant dependence of on microstructural parameters is contained in the term ϕ [24]. For creep and densification by lattice diffusion, transport of matter occurs from grain boundaries under compression and grain boundaries under tension to adjacent pores. The constants K_1 and K_2 in Equation 5 were considered to be approximately equal so that

$$\Sigma = \left(\frac{\dot{\varrho}}{3\varrho\dot{\varepsilon}}\right)\sigma_a\phi \quad (6)$$

The magnitude of the effective sintering stress can then be found from Equation 6, and is shown in Fig. 11 as a function of ϱ. The value of Σ decreases from ~ 20 MPa at $\varrho = 0.55$ to ~ 5 MPa at $\varrho = 0.85$. Since the grain size, G, increases by a factor of $\leqslant 2$ over this density range, the decrease in Σ can be explained almost entirely as due to the change in ϕ with porosity.

5. Conclusions

The loading dilatometer technique has been used to study the simultaneous creep and densification behaviour of ZnO powder compacts and the results were compared with those obtained earlier for an oxide ceramic, CdO, and a glass. The general trends in the results were similar to those for CdO but some important differences were observed.

The stress intensification factor, ϕ, was found to have an exponential dependence on porosity, P, of the form $\phi \sim \exp(aP)$, where a is a constant equal to 5. Although this expression is functionally similar to that for CdO, it showed a stronger dependence on porosity for approximately the same dihedral angle.

The sintering effective stress, Σ, was found to decrease with increasing density, but this decrease can be entirely explained as due to the change of ϕ with porosity.

The ratio of the linear densification rate to the creep rate was nearly constant over a wide range of density between 0.55 and 0.85. Similar behaviour has been observed for CdO and glass, although the actual magnitude of this ratio varied significantly for the different materials.

Acknowledgement

This work was supported by the Division of Materials Sciences, Office of Basic Energy Sciences, US Department of Energy, under Contract No. DE-AC03-76SF00098.

References

1. A. G. EVANS, *J. Amer. Ceram. Soc.* **65** (1982) 497.
2. R. RAJ and R. K. BORDIA, *Acta Metall.* **32** (1984) 1003.
3. L. C. DE JONGHE, M. N. RAHAMAN and C-H. HSUEH, *ibid.* **34** (1986) 1467.
4. C-H. HSUEH, A. G. EVANS and R. M. McMEEKING, *J. Amer. Ceram. Soc.* **69** (1986) C-64.
5. L. C. DE JONGHE and M. N. RAHAMAN, *Rev. Sci. Instrum.* **55** (1984) 2010.
6. M. N. RAHAMAN and L. C. DE JONGHE, *J. Amer. Ceram. Soc.* **67** (1984) C-205.
7. M. N. RAHAMAN, L. C. DE JONGHE and R. J. BROOK, *ibid.* **69** (1986) 53.
8. M. N. RAHAMAN, L. C. DE JONGHE and R. J. BROOK, *ibid.* (1987).
9. R. L. COBLE, *J. Appl. Phys.* **41** (1970) 4798.
10. W. BEERE, *Acta Metall.* **23** (1975) 131.
11. *Idem, ibid.* **23** (1975) 139.
12. J. M. VIEIRA and R. J. BROOK, *J. Amer. Ceram. Soc.* **67** (1984) 245.
13. R. A. GREGG and F. N. RHINES, *Metall. Trans.* **4** (1973) 1365.
14. E. H. AIGELTINGER, *Int. J. Powder Metall. Powder Technol.* **11** (1975) 195.
15. M. LIN, M. N. RAHAMAN and L. C. DE JONGHE, *J. Amer. Ceram. Soc.*
16. K. R. VENKATACHARI and R. RAJ, *ibid.* **69** (1986) 499.
17. R. K. BORDIA and R. RAJ, *ibid.* **69** (1986) C-55.
18. M. N. RAHAMAN and L. C. DE JONGHE, unpublished work.
19. R. RAJ, *J. Amer. Ceram. Soc.* **65** (1982) C-46.
20. F. R. N. NABARRO, in Report on the Conference on Strength of Solids (Bristol, 1947, 1948) p. 75.
21. C. HERRING, *J. Appl. Phys.* **21** (1950) 437.
22. R. L. COBLE, *ibid.* **34** (1963) 1679.
23. T. K. GUPTA and R. L. COBLE, *J. Amer. Ceram. Soc.* **51** (1968) 521.
24. L. C. DE JONGHE and M. N. RAHAMAN, *Acta Metall.* (1987).

Received 12 January
and accepted 1 April 1987